P78-2 SCATHA ENVIRONMENTAL DATA ATLAS

E. Gary Mullen and David A. Hardy
Air Force Geophysics Laboratory

Henry B. Garrett
Jet Propulsion Laboratory
California Institute of Technology

Elden C. Whipple
University of California at San Diego

SUMMARY

A study of the 100 eV to ~1 MeV plasma environment encountered by the P78-2 Spacecraft Charging at High Altitudes (SCATHA) satellite during its initial operation period was conducted. Forty-four days of 10-minute averages of the 4 moments of the electron and ion distribution functions calculated from the SC5 and SC9 energetic particle measurements were analyzed to determine occurrence frequency, local time variation, geomagnetic activity variation, and L-shell variation. The single and double Maxwellian parameters derived from the 4 moments were similarly analyzed. The interrelationships between the moments and derived parameters were computed and the results compared with the ATS-5 and ATS-6 atlas of Garrett et al. (references 4,5). Results of this analysis establish a baseline range for the SCATHA plasma environment.

INTRODUCTION

A preliminary study of the 100 eV to ~1 MeV plasma environment encountered by the P78-2 Spacecraft Charging at High Altitudes (SCATHA) satellite during its initial operation period has been completed. As reported previously (references 1, 2, 3, 4 and 5), a similar analysis was carried out for the ATS-5 and ATS-6 geosynchronous plasma data. The purpose of this paper is to summarize the findings of these studies and to compare the different data bases. The details of the P78-2, ATS-5, and ATS-6 plasma studies are to be found principally in Mullen et al. (reference 6) and Garrett et al. (references 2, 3, 4 and 5).

DATA BASE

Our current understanding of the statistical variations in the geosynchronous and near-geosynchronous plasma environments derives primarily from the University of California (UCSD) plasma experiments on ATS-5 and ATS-6. The recent launch of the P78-2 satellite has allowed an expansion of this data base as P78-2 flew a UCSD instrument, SC9, identical to those flown on ATS-5 and ATS-6. The diversity of instrumentation on P78-2 has also allowed an intercomparison with a different instrument, SC5, flown by the Air Force Geophysics Laboratory (AFGL). To accomplish this intercomparison, the differential spectra returned by the instruments were integrated to give the 4 moments of the electron and ion distribution functions and estimates of the Maxwellian and 2 Maxwellian temperatures (reference 1). These were combined to give 10 minute averages. These 10 minute averages (approximately 50 days for each instrument) were analyzed statistically in terms of average values, histograms, variations in geomagnetic activity and local time, and interrelationships between parameters. The elliptical orbit of P78-2 also allowed an analysis in terms or radial variations. The instruments will be briefly described below with the variations being discussed in a subsequent section.

The UCSD plasma detectors are described in DeForest and McIlwain (1971)[7] (ATS-5), Mauk and McIlwain (1975)[8] (ATS-6), and Stevens and Vampola (1978)[9] (P78-2). These instruments are similar except for energy range and accumulation time. All 3 instruments consist of pairs of electrostatic analyzers designed to measure the positive ion and electron populations between 51 eV and 51 KeV (ATS-5) or 1 eV and 80 KeV (ATS-6 and P78-2). The ATS-5 detectors measured fluxes parallel and perpendicular to the satellite spin axis whereas ATS-6 and SC9 can scan in the north-south and east-west meridians. ATS-5 returns a complete 64-step spectrum in 20 seconds and ATS-6 and SC9 in 15 seconds.

SC5 (Hanser et al, 1979)[10] is designed to sample the electron and ion fluxes at ~1 second time intervals over a very large energy range (~50 eV - .5 MeV). This energy range necessitates a unique design involving both electrostatic and solid state detectors. The detectors are mounted parallel and perpendicular to the satellite spin axis (only those parallel to the axis were used in this study).

As outlined in Garrett et al. (references 4 and 5) and Mullen et al. (reference 6), there are several constraints on the data base. Summarizing:

1) Angular effects - the data have been assumed for the preliminary analysis to be isotropic.

2) The ions are assumed to be H^+.

3) Spacecraft charging has not been corrected in the P78-2 data.

4) The energy ranges of ATS-6 electrons, SC5 electrons and ions, and SC9 electrons and ions were cut off below 100 eV (ATS-5 was left at 50 eV).

5) The high energy cut-offs of ATS-5, ATS-6, and SC9 are considerably lower than SC5. An attempt has been made to correct for this effect by extrapolating the data assuming

Maxwellian distributions but a difference is still noticeable in the data.

6) At the time of this paper, the SC5 and SC9 data were still being calibrated (Hardy, private communication) so that the P78-2 data must be considered preliminary.

The above effects, while important, are believed to be acceptable given the order of plasma variations (factors of ~100) and the large statistical samples considered (typically 6000 10-minute averages per instrument). It is intended that the final SCATHA atlas will correct these deficiencies (see Table 5).

ATS-5, ATS-6, AND P78-2 INTERCOMPARISONS

Rather than repeat the extensive analysis of the ATS-5, ATS-6, and P78-2 to be found in Garrett (reference 1), Garrett et al. (references 2, 3, 4 and 5), and Mullen et al. (reference 6), this section will present selected examples from that analyses. As the most important parameters for spacecraft charging are the current (J) and Maxwellian temperature, our examples will be confined to these 2 parameters. We have chosen to present the temperature of the high energy 2 Maxwellian component, T2 (see reference 1). The variations in J are representative of those in the other moments while T2 is representative of TAVG and TRMS (there are important exceptions, however, and the reports cited above should be consulted).

The basic analysis consisted of calculating the averages of the various moments, the 2 Maxwellian components, and TAVG and TRMS. These averages are listed in Table 1 for the electrons and ions. For completeness, we have also listed the standard deviations (Table 2) but as in most cases the data did not follow a Gaussian distribution, they have limited meaning. Typically the averages of the moments are all in reasonably close agreement with ATS-5 having the lowest values. This is also observed in the temperatures although the differences are much larger (note that $T2_e$ is twice the other values for SC5 - we believe this to be an instrumental effect - see later).

Histograms have been prepared of all the variables. Figure 1 is a histogram of the occurrence frequency of Kp for ATS-5, ATS-6 and P78-2. The P78-2 intervals fall between the ATS-5 and ATS-6 intervals implying that P78-2 saw geomagnetic conditions in between ATS-5 and ATS-6. Likewise, the P78-2 data fall in between ATS-5 and ATS-6 data in the histograms in Figure 2. The major differences in these histograms are between $T2_e$ for SC5 and the other instruments and between $T2_I$ for ATS-6 and the other instruments. The SC5 variation we believe results from the fact that SC5 can record much higher energy particles than the other instruments.

The ATS-6 difference is consistent with the average increase in geomagnetic activity observed by ATS-6 (Figure 1). In any case, these histograms demonstrate good agreement between the instruments and give the engineer a quantitative measure of the parameter ranges to be expected.

In Figure 3 we have plotted the average variations in local time of J and T2. The local time variations in the current are in excellent agreement between the instruments. For $T2_e$ and to somewhat of a lesser degree for $T2_I$, the SC5 data depart dramatically from the UCSD data. We again attribute this to the difference in instrument energy ranges. Further, the P78-2 data are biased in radial distance - local time (see Table 3). Even so, the data imply a pronounced minimum in the electron current near 16 LT and a weak maximum (except for SC5) in $T2_e$ in the same LT range. As charging is believed to maximize near midnight, these results may imply that it is changes in the electron current that are the primary source of changes in the charging level at geosynchronous orbit.

Also plotted in Figure 3 are the average variations with Kp. Again the 4 instruments are similar except for $T2_e$ as recorded by SC5 (the trend for $T2_e$, however, is consistent). First, the T2 parameters show little or no increase with Kp. Secondly, the largest increase with Kp is the electron current. There is only a weak increase for the ions. Again this implies that most of the average change at geosynchronous orbit is in the electron current.

The final variation to be discussed is in radial distance or in normalized L-shell coordinates. The SC5 and SC9 variations in L-shell (where L=1 is roughly the radius of the earth) are plotted in Figure 4. Note the non-existent variation in J_e and the sharp decrease in J_I with increasing L (Note: J_e is in nA-cm^{-2} and J_I in 10^{-2}nA-cm^{-2}). Both $T2_e$ and $T2_I$ decrease with increasing L (again, the difference between SC5 and SC9 is believed to be instrumental). Such variations could not be studied with ATS-5 and ATS-6 and indicate the importance of the P78-2 data in better defining the geosynchronous environment.

CONCLUSION

The ATS-5, ATS-6, and P78-2 statistical atlas results have been compared in terms of the parameters J and T2. Inspite of differences in geomagnetic activity and instrumentation (SC5 versus the UCSD detectors), the different statistical populations are in good agreement. Taken together, they give a strong validation of the current statistical data base established for the geosynchronous plasma.

The justification for studying the P78-2 data is clearly revealed by the comparisons presented here. First, the ATS-5, ATS-6, and SC9 instruments yield consistent results validating our faith in their reliability overtime. They demonstrate the role of geomagnetic and local time variations and point toward the importance of variations in the current. The differences between the ion temperatures measured by ATS-5, ATS-6, and SC9 also imply long-term variations in the state of the geosynchronous plasma. The SC5 data demonstrate that care must be taken in analyzing a limited energy range - the entire energy spectrum from ~0 to 1 MeV may turn out to be important to charging. Future studies should, when possible, include plasma data above 100 KeV. Finally, the P78-2 has allowed an evaluation of radial variations that was impossible with ATS-5 and ATS-6. The data imply strong radial gradients that must be considered in spacecraft charging studies.

In spite of the successes of the preliminary P78-2 atlas, a number of issues remain unresolved. These areas are to be filled in by the final P78-2 atlas. The major areas are listed in Table 5. The preliminary atlas was intended to provide an initial answer to these problems and a baseline for the P78-2. At the same time, it was to provide a confirmation of the validity of the ATS-5 and ATS-6 atlas. These goals, as demonstrated here, have been met.

REFERENCES

1. Garrett, H. B.: Modeling of the Geosynchronous Plasma Environment. Spacecraft Charging Technology, 1978. NASA CP-2071/AFGL-TR-79-0082, 1979, pp. 11-22.

2. Garrett, H. B.; Mullen, E.G.; Ziemba, E.; and DeForest, S.E.: Modeling of the Geosynchronous Plasma Environment - Part 2. ATS-5 and ATS-6 Statistical Atlas. AFGL-TR-78-0304, 1978.

3. Garrett, H. B.; McInerney, R.E.; DeForest, S. E.; and Johnson, B.: Modeling of the Geosynchronous Orbit Plasma Environment - Part 3, ATS-5 and ATS-6 Pictorial Data Atlas. AFGL-TR-79-0015, 1979.

4. Garrett, H. B.; Schwank, D. C.; and DeForest, S. E.: A Statistical Analysis of the Low Energy Geosynchronous Plasma Environment. Part I - Electrons. Submitted to Planet. Space Sci., 1980.

5. Garrett, H. B.; Schwank, D. C.; and DeForest, S. E.: A Statistical Analysis of the Low Energy Geosynchronous Plasma Environment. Part II - Ions. Submitted to Planet Space Sci., 1980.

6. Mullen, E. G.; Garrett, H. B.; Hardy, D. A.; and Whipple, E. C.: P78-2 SCATHA Environmental Data Atlas. AFGL-TR-80-0241,1980.

7. DeForest, S. E.; and McIlwain, C.E.: Plasma Clouds in the Magnetosphere. J. Geophys. Res., 76, 1979, pp. 3587-3611.

8. Mauk, B. H.; and McIlwain, C. E.: ATS-6 Auroral particle experiment. IEEE Trans. Aerospace and Electronics Systems, AEA-11 (No. 6), 1975, pp. 1125-1130.

9. Stevens, J. R.; and A. L. Vampola: Description of the Space Test Program P78-2 Spacecraft and Payloads. SAMSO-TR-78-24, 1978; pp. 49-53.

10. Hanser, F. A.; Hardy, D. A.; and Sellers, B.: Calibration of the Rapid Scan Particle Detector Mounted in the SCATHA Satellite. AFGL-TR-79-0167, 1979.

TABLE 1a. AVERAGES (ELECTRONS)

PARAMETER	ATS-5	ATS-6	SC9	SC5
ND (cm^{-3})	.80	1.06	1.09	.82
J ($nA\text{-}cm^{-2}$)	.068	.096	.115	.086
ED ($eV\text{-}cm^{-3}$)	1970	3590	3710	3240
EF ($eV\text{-}cm^{-2}\text{-}s^{-1}\text{-}sr^{-1}$)	$.98 \times 10^{12}$	2.17×10^{12}	1.99×10^{12}	2.26×10^{12}
N1 (cm^{-3})	.578	.751	.780	.654
T1 (KeV)	.277	.460	.550	.725
N2 (cm^{-3})	.215	.273	.310	.169
T2 (KeV)	7.04	9.67	8.68	17.4
TAVG (KeV)	1.85	2.55	2.49	3.20
TRMS (KeV)	3.85	6.25	4.83	8.26

TABLE 1b. AVERAGES (IONS)

PARAMETER	ATS-5	ATS-6	SC9	SC5
ND (cm^{-3})	1.30	1.20	.58	.69
J ($pA\text{-}cm^{-2}$)	5.1	3.4	3.3	4.1
ED ($eV\text{-}cm^{-3}$)	13000	12000	9440	12400
EF ($eV\text{-}cm^{-2}\text{-}s^{-1}\text{-}sr^{-1}$)	2.6×10^{11}	3.4×10^{11}	2.0×10^{11}	2.93×10^{11}
N1 (cm^{-3})	.75	.93	.19	.33
T1 (KeV)	.30	.27	.80	2.13
N2 (cm^{-3})	.61	.33	.39	.36
T2 (KeV)	14.0	25.0	15.8	21.1
TAVG (KeV)	6.8	12.0	11.2	12.1
TRMS (KeV)	12.0	23.0	14.5	16.8

TABLE 2a. STANDARD DEVIATIONS (ELECTRONS)

PARAMETER	ATS-5	ATS-6	SC9	SC5
ND (cm^{-3})	$\pm.79$	±1.1	$\pm.89$	$\pm.75$
J ($nA\text{-}cm^{-2}$)	$\pm.088$	$\pm$ .09	$\pm.10$	$\pm.08$
ED ($eV\text{-}cm^{-3}$)	±3100	±3700	±3400	±3300
EF ($eV\text{-}cm^{-2}\text{-}s^{-1}\text{-}sr^{-1}$)	$\pm1.7 \times 10^{12}$	$\pm2.6 \times 10^{12}$	$\pm2.0 \times 10^{12}$	$\pm2.29 \times 10^{12}$
N1 (cm^{-3})	$\pm.55$	$\pm.82$	$\pm.70$	$\pm.60$
T1 (KeV)	$\pm.17$	$\pm.85$	$\pm.32$	$\pm.66$
N2 (cm^{-3})	$\pm.38$	$\pm.34$	$\pm.37$	$\pm.23$
T2 (KeV)	±2.1	±3.6	±4.0	±11
TAVG (KeV)	±2.0	±2.0	±1.5	±2.7
TRMS (KeV)	±3.3	±3.5	±2.9	±5.8

TABLE 2b. STANDARD DEVIATIONS (IONS)

PARAMETER	ATS-5	ATS-6	SC9	SC5
ND (cm^{-3})	$\pm.69$	±1.7	$\pm.35$	$\pm.41$
J ($pA\text{-}cm^{-2}$)	±2.7	±1.8	±2.1	±2.6
ED ($eV\text{-}cm^{-3}$)	±9700	±9100	±6820	±8900
EF ($eV\text{-}cm^{-2}\text{-}s^{-1}\text{-}sr^{-1}$)	$\pm3.5 \times 10^{11}$	$\pm3.6 \times 10^{11}$	$\pm1.7 \times 10^{11}$	$\pm2.5 \times 10^{11}$
N1 (cm^{-3})	$\pm.54$	±1.78	$\pm.16$	$\pm.24$
T1 (KeV)	$\pm.30$	$\pm.88$	±1.0	±1.4
N2 (cm^{-3})	$\pm.33$	$\pm.16$	$\pm.26$	$\pm.24$
T2 (KeV)	±5.0	±8.5	±5.0	±8.7
TAVG (KeV)	±3.6	±8.4	±4.6	±5.2
TRMS (KeV)	±4.8	±8.9	±5.3	±7.1

TABLE 3

P78-2 10 MINUTE INTERVALS
IN A GIVEN LOCAL TIME/L SHELL INTERVAL

	5.5	6.0	5.5	7.0	7.5	8.0	8.5	TOTAL
TOTAL	375	250	454	611	667	352	111	2920
21-24	59	18	6	17	75	94	52	321
18-21	81	16	53	76	42	22	0	290
15-18	38	65	11	0	0	10	10	134
12-15	61	42	85	18	1	0	4	211
9-12	75	46	77	184	59	0	0	441
6-9	56	96	66	109	319	5	0	651
3-6	0	4	109	196	145	70	7	531
0-3	5	63	47	11	26	151	38	341

L SHELL

TABLE 4

P78-2 10 MINUTE INTERVALS
IN A GIVEN Kp/L SHELL INTERVAL

TOTAL	375	250	454	611	667	352	111	2920
5+	10	14	6	17	37	0	4	88
4+	57	31	35	38	96	32	3	292
3+	119	88	83	107	139	81	30	647
2+	100	99	155	205	171	117	41	888
1+	57	69	108	159	121	85	19	618
0+	32	49	67	85	103	37	14	387
	5.5	6.0	6.5	7.0	7.5	8.0	8.5	TOTAL

L SHELL

TABLE 5. PROPOSED FINAL ATLAS CONTENTS

Statistical variations of energetic particle fluxes as functions of Kp L-shell and local time.

Average particle distribution functions and ranges of individual distributions to include worst case.

Distribution functions during charging events.

Pitch angle distribution of particles during quiet and charging periods.

Spectrograms.

Ion composition data.

Electric and magnetic fields.

Supplemental data from Geos and other satellites.

Section on plasma dropouts and injection events and their relationship to charging.

Identify regions and conditions for maximum probability of charging.

Determine best fits to particle distribution functions whether physical or empirical for model use.

Simplified "worst case" environment.

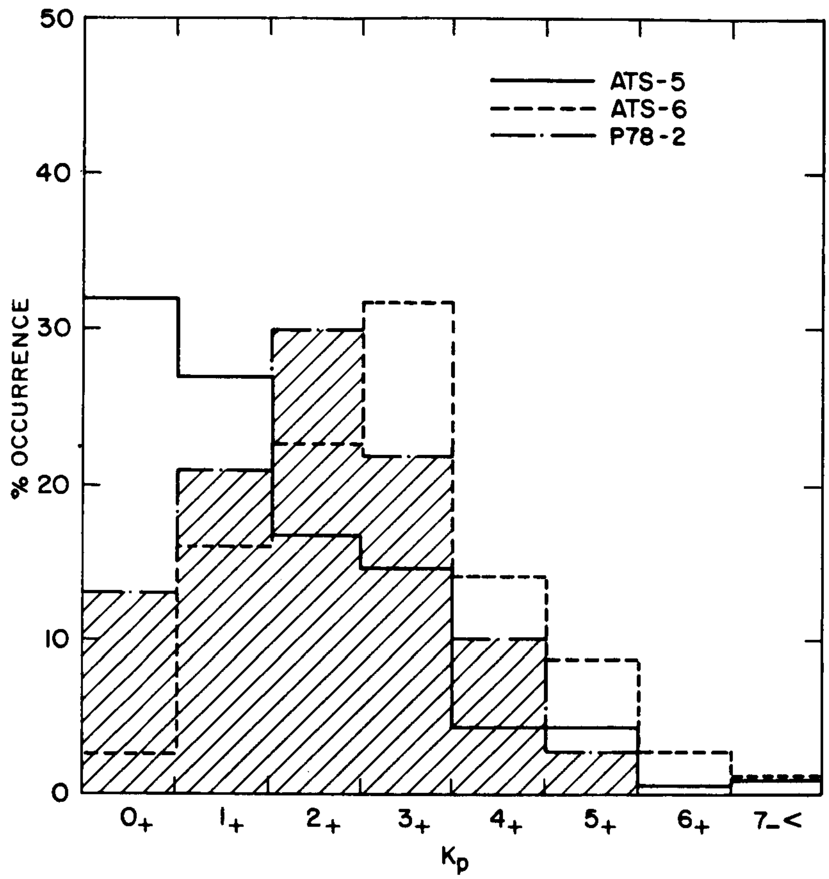

Figure 1. - Occurrence frequency of K_p for ATS-5, ATS-6, and P78-2 satellites.

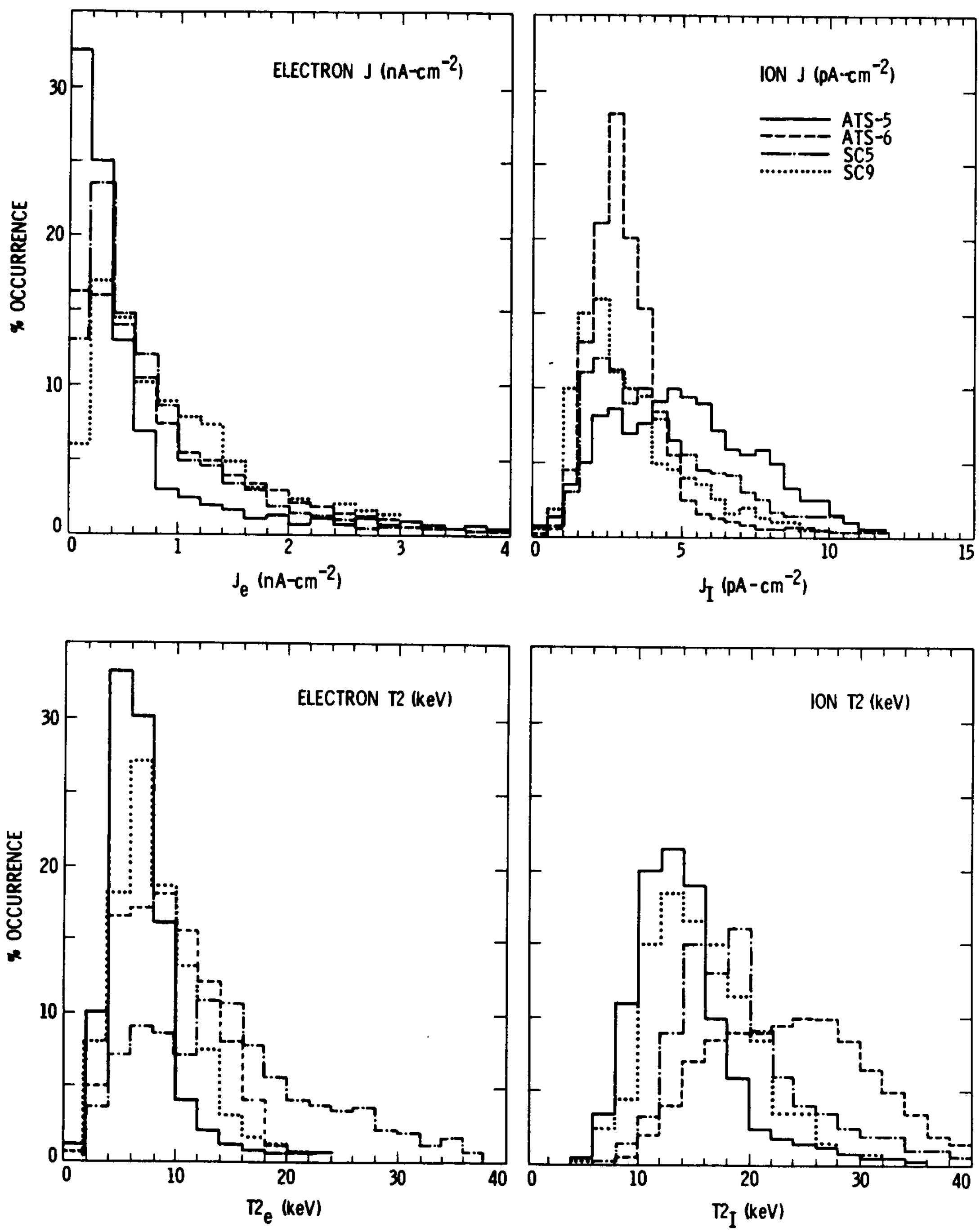

Figure 2. - Histograms of current density J and 2 Maxwellian temperature T2 for ATS-5, ATS-6, and P78-2.

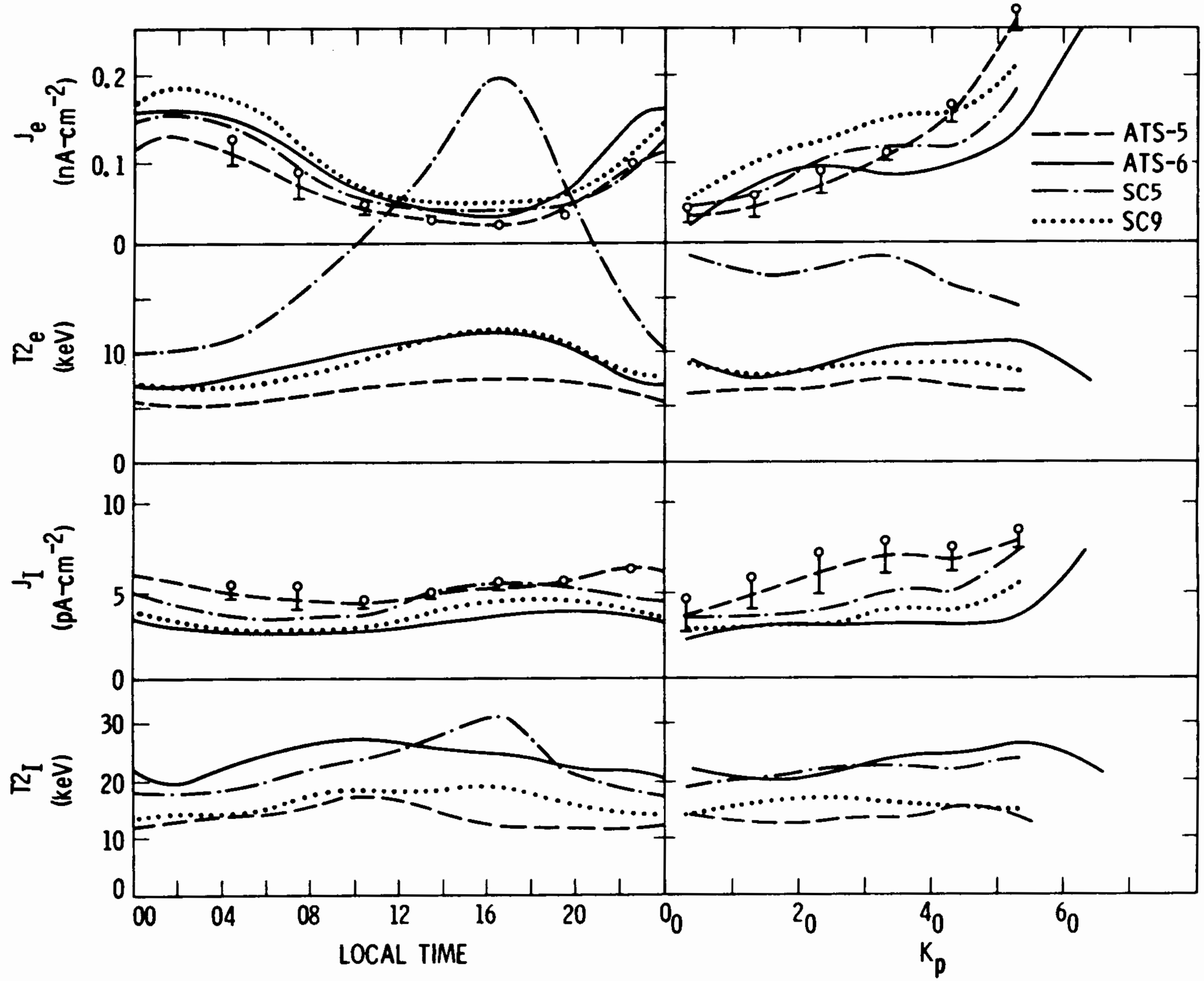

Figure 3. - Plots of average local time and K_p variations observed by ATS-5, ATS-6, and P78-2. Error bars correspond to average variations of ATS-5 parallel (-) and perpendicular (0) detectors.

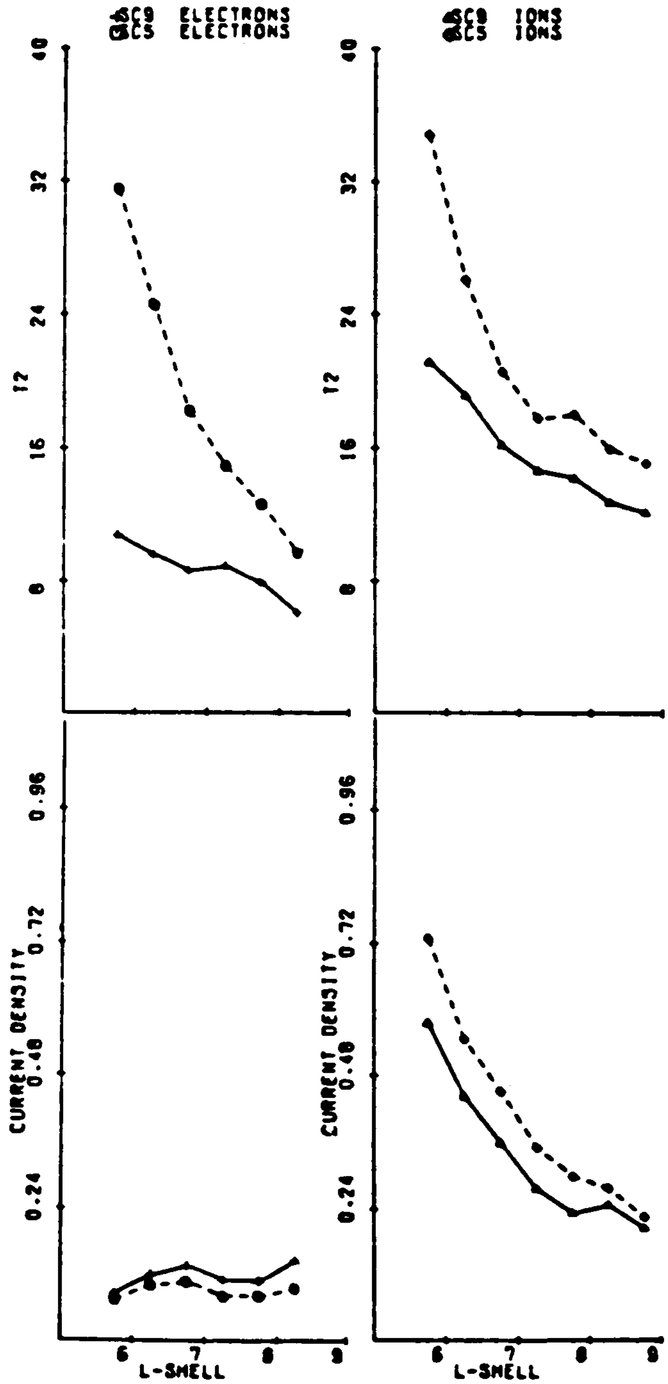

Figure 4. - Plots of variations with L-shell of parameters J (current density) and T2 (2 Maxwellian temperature component). Current density is in units of nA cm^{-2} for electrons and 10^{-2} nA cm^{-2} for ions. T2 is in units for keV.